

ICA Using Spacings Estimates of Entropy

Erik G. Learned-Miller

EGMIL@EECS.BERKELEY.EDU

*Department of Electrical Engineering and Computer Science
University of California
Berkeley, CA 94720-1776, USA*

John W. Fisher III

FISHER@CSAIL.MIT.EDU

*Computer Science and Artificial Intelligence Laboratory
Massachusetts Institute of Technology
200 Technology Square, Office NE43-V 626
Cambridge MA 02139, USA*

Editors: Te-Won Lee, Jean-François Cardoso, Erkki Oja and Shun-ichi Amari

Abstract

This paper presents a new algorithm for the independent components analysis (ICA) problem based on an efficient entropy estimator. Like many previous methods, this algorithm directly minimizes the measure of departure from independence according to the estimated Kullback-Leibler divergence between the joint distribution and the product of the marginal distributions. We pair this approach with efficient entropy estimators from the statistics literature. In particular, the entropy estimator we use is consistent and exhibits rapid convergence. The algorithm based on this estimator is simple, computationally efficient, intuitively appealing, and outperforms other well known algorithms. In addition, the estimator's relative insensitivity to outliers translates into superior performance by our ICA algorithm on outlier tests. We present favorable comparisons to the Kernel ICA, FAST-ICA, JADE, and extended Infomax algorithms in extensive simulations. We also provide public domain source code for our algorithms.

1. Introduction

We present a new independent components analysis (ICA) algorithm, RADICAL. Empirical results indicate that it outperforms a wide array of well known algorithms. Several straightforward principles underly the development of RADICAL:

1. Since ICA is, by definition, about maximizing statistical independence, we attempt to directly optimize a measure of statistical independence, rather than a surrogate for this measure.
2. We avoid explicit estimation of probability densities as an intermediate step. Indeed, given the formulation of the objective function, density estimation (even implicitly) is entirely unnecessary.
3. Since our objective function involves one-dimensional entropy estimation, we employ a well-known,¹ consistent, rapidly converging and computationally efficient estimator of entropy

1. Although the estimator that we use (Vasicek, 1976) has been extensively analyzed in the statistics literature, it has received little attention in the machine learning community.

which is robust to outliers. For this task, we turned to the statistics literature, where entropy estimators have been studied extensively (c.f. Beirlant et al., 1997).

4. As the optimization landscape has potentially many local minima, we eschew gradient descent methods. The fact that the estimator is computationally efficient allows for a global search method. The structure of the ICA problem allows for extension of this technique to higher dimensions in a tractable manner.

Attention to these principles led to the Robust, Accurate, Direct ICA aLgorithm (RADICAL) presented here. Implementations of the RADICAL program can be found on the first author's home page, at the web address <http://www.eecs.berkeley.edu/~egmil/ICA>. At the time of publication, all of the source code was in MATLAB.

The paper is organized as follows. We begin by setting up the problem and discussing aspects of the contrast function originally proposed by Comon (1994), which can be simplified to a sum of one-dimensional marginal entropies (c.f. Kullback, 1959). In Section 2, we discuss entropy estimates based on order statistics. One method in particular satisfies our requirements, the *m-spacing* estimator (Vasicek, 1976).

This entropy estimator leads naturally to a simple ICA algorithm, a two-dimensional version of which is described in Section 3. We follow this with a discussion of complexity and experimental results for the two-dimensional problem. In addition to working for a wide variety of possible source distributions, we demonstrate that RADICAL has excellent robustness to the presence of outliers. In Section 4, we extend the algorithm to higher dimensional problems, with experiments in up to 16 dimensions. We discuss additional details of the algorithm and discuss why the complexity is still manageable, even using our exhaustive search approach.

1.1 Linear ICA and Kullback-Leibler Divergence

As articulated by Comon (1994), ICA applied to instantaneous linear mixtures considers the generative model of random observations

$$X = AS.$$

Here $X \in \mathfrak{R}^C$ and $S \in \mathfrak{R}^D$ are random vectors, and $A \in \mathfrak{R}^{C \times D}$ is a fixed but unknown. Because A is unknown, this problem is also referred to as *blind source separation*, where the components of S are the original sources. Typically, at a minimum, one assumes that

1. The mixing matrix A has full rank;
2. The components of S are mutually independent; and
3. $C \geq D$.

Condition 2 is equivalent to the statement that the joint density of the components of S can be expressed as a product of the marginals:

$$p(S_1, \dots, S_D) = \prod_{i=1}^D p(S_i).$$

Additionally, here we shall restrict ourselves to the case where A is square, without loss of generality. The goal is to recover (in some sense) the set of sources S_1, S_2, \dots, S_N and perhaps the mixing matrix

via a transformation W on observations of X , that is

$$\begin{aligned} Y &= WX \\ &= WAS \\ &= BS. \end{aligned}$$

Given the minimal statement of the problem, it has been shown (Benveniste et al., 1980, Comon, 1994) that one can recover the original sources up to a scaling and permutation provided that at most one of the underlying sources is Gaussian and the rest are non-Gaussian. Upon pre-whitening the observed data the problem reduces to a search over rotation matrices in order to recover the sources and mixing matrix in the sense described above (Hyvärinen, 2001, Bach and Jordan, 2002). We will assume henceforth that such pre-processing has been done.

While the problem statement is fairly straightforward with a minimum of assumptions it has been well studied, resulting in a vast array of approaches. Some of the more notable approaches can be roughly grouped into maximum likelihood based methods (Pham et al., 1992, Pearlmutter and Parra, 1996), moment/cumulant based methods (Comon, 1994, Cardoso and Souloumiac, 1996, Cardoso, 1999a, Hyvärinen, 2001), entropy based methods (Bell and Sejnowski, 1995, Hyvärinen, 1999, Bercher and Vignat, 2000), and correlation based methods (Jutten and Herault, 1991, Bach and Jordan, 2002).

Many approaches start the analysis of the problem by considering the contrast function (Comon, 1994)

$$\begin{aligned} J(Y) &= \int p(y_1, \dots, y_D) \log \frac{p(y_1, \dots, y_D)}{p(y_1)p(y_2)\dots p(y_D)} d\mu & (1) \\ &= KL \left(p(y_1, \dots, y_D) \parallel \prod_{i=1}^D p(y_i) \right) \\ &= \sum_{i=1}^D H(Y_i) - H(Y_1, \dots, Y_D). \end{aligned}$$

Here $d\mu = dy_1 dy_2 \dots dy_D$ and $H(Y)$ is the differential entropy (Shannon, 1948) of the continuous multi-dimensional random variable Y . The right side of (1) is the Kullback-Leibler divergence (Kullback, 1959), or relative entropy, between the joint density of $\{Y_1, \dots, Y_D\}$ and the product of its marginals.

The utility of (1) for purposes of the ICA problem has been well documented in the literature (c.f. Comon, 1994, Lee et al., 1999a). Briefly, we note that for mutually independent random variables Y_1, Y_2, \dots, Y_D we have

$$\begin{aligned} J(Y) &= \int p(y_1, y_2, \dots, y_D) \log \frac{p(y_1, y_2, \dots, y_D)}{p(y_1)p(y_2)\dots p(y_D)} d\mu \\ &= \int p(y_1, y_2, \dots, y_D) \log 1 d\mu \\ &= 0. \end{aligned}$$

Since this quantity will be 0 if and only if all of the variables are *mutually independent*, we take (1) as a direct measure of mutual independence.

As a function of X and W it is easily shown (c.f. Cover and Thomas, 1991) that

$$J(Y) = \sum_{i=1}^D H(Y_i) - H(X_1, \dots, X_D) - \log(|W|).$$

In particular, the change in the entropy of the joint distribution under linear transformation is simply the logarithm of the Jacobian of the transformation. As we will assume the X 's are pre-whitened, W will be restricted to rotation matrices, for which $\log(|W|) = 0$, and the minimization of $J(Y)$ reduces to finding

$$W^* = \arg \min_W H(Y_1) + \dots + H(Y_D). \quad (2)$$

The preceding development brings us to the primary contribution of this paper. As has been noted (Hyvärinen, 1999), ICA algorithms consist of an objective (contrast) function *and* an optimization algorithm. We adopt the previously proposed objective criterion of (2) and present a means of both estimating its value and optimizing the choice of W in a reliable, robust, and computationally efficient method. These aspects of our approach are the subject of the rest of the paper.

Towards that end, we adopt a different entropy estimator to minimize (2). The entropy estimator is almost identical to one described by Vasicek (1976) and others (c.f. Beirlant et al., 1997, for a review) in the statistics literature. This class of entropy estimators has not heretofore been applied to the ICA problem. As we will show, the use of this entropy estimator has a significant impact on performance as compared to other ICA algorithms and as discussed in the section on experimental results. In addition, it has the following desirable properties:

- It is consistent.
- It is asymptotically efficient, with square root of N convergence (where N is the number of data points).
- It is computable in $O(N \log N)$ time.

In the next section, we present a detailed discussion of the entropy estimator and its properties.

2. Entropy Estimators for Continuous Random Variables

There are a variety of ICA algorithms that minimize (2) to find the independent components (e.g. Comon, 1994). These algorithms differ mostly in how they estimate the entropy of the one-dimensional marginal variables. Hyvärinen (1997), for example, developed a new entropy estimator for this purpose. RADICAL also uses entropy minimization at its core, and as such must estimate the entropy of each marginal for each possible W matrix. RADICAL's marginal entropy estimates are functions of the *order statistics* of those marginals.

2.1 Order Statistics and Spacings

Consider a one-dimensional random variable Z , and a random sample of Z denoted by Z^1, Z^2, \dots, Z^N . The *order statistics* of a random sample of Z are simply the elements of the sample rearranged in non-decreasing order: $Z^{(1)} \leq Z^{(2)} \leq \dots \leq Z^{(N)}$ (c.f. Arnold et al., 1992). A *spacing of order m* , or *m -spacing*, is then defined to be $Z^{(i+m)} - Z^{(i)}$, for $1 \leq i < i+m \leq N$. Finally, if m is a function of N , one may define the *m_N -spacing* as $Z^{(i+m_N)} - Z^{(i)}$.

The m_N -spacing estimator of entropy, originally due to Vasicek (1976), can now be defined as

$$\hat{H}_N(Z^1, Z^2, \dots, Z^N) = \frac{1}{N} \sum_{i=1}^{N-m_N} \log \left(\frac{N}{m_N} (Z^{(i+m_N)} - Z^{(i)}) \right). \quad (3)$$

This estimator is nearly equivalent to the one used in RADICAL, which is discussed below. To see where this estimator comes from, we first make the following observation regarding order statistics. For any random variable Z with an impulse-free density $p(\cdot)$ and continuous distribution function $P(\cdot)$, the following holds. Let p^* be the N -way product density $p^*(Z^1, Z^2, \dots, Z^N) = p(Z^1)p(Z^2)\dots p(Z^N)$. Then

$$E_{p^*}[P(Z^{(i+1)}) - P(Z^{(i)})] = \frac{1}{N+1}, \quad \forall i, 1 \leq i \leq N-1. \quad (4)$$

That is, the expected value of the probability mass of the interval between two successive elements of a sample from a random variable is just $\frac{1}{N+1}$ of the total probability (which by definition must be equal to 1.0).² This surprisingly general fact is a simple consequence of the uniformity of the random variable $P(Z)$. $P(Z)$, the random variable describing the “height” on the cumulative curve of a random draw from Z (as opposed to the function $P(z)$) is called the *probability integral transform* of Z (c.f. Manoukian, 1986). Thus, the key insight is that the *intervals* between successive order statistics have the same expected probability mass.

Using this idea, one can develop a simple entropy estimator. We start by approximating the probability density $p(z)$ by assigning equivalent masses to each interval between points and assuming a uniform distribution of this mass across the interval.³ Defining $Z^{(0)}$ to be the infimum of the support of $p(z)$ and defining $Z^{(N+1)}$ to be the supremum of the support of $p(z)$, we have

$$\hat{p}(z; Z^1, \dots, Z^N) = \frac{\frac{1}{N+1}}{Z^{(i+1)} - Z^{(i)}}$$

2. The probability mass of the interval between two successive points can also be thought of as the integral of the density function between these two points.

3. We use the notion of a density estimate to aid in the intuition behind m -spacing estimates of entropy. However, we stress that density estimation *is not* a necessary intermediate step in entropy estimation.

for $Z^{(i)} \leq z < Z^{(i+1)}$. Then, we can write

$$\begin{aligned}
 H(Z) &= - \int_{-\infty}^{\infty} p(z) \log p(z) dz \\
 &\stackrel{(a)}{\approx} - \int_{-\infty}^{\infty} \hat{p}(z) \log \hat{p}(z) dz \\
 &= - \sum_{i=0}^N \int_{Z^{(i)}}^{Z^{(i+1)}} \hat{p}(z) \log \hat{p}(z) dz \\
 &= - \sum_{i=0}^N \int_{Z^{(i)}}^{Z^{(i+1)}} \frac{1}{Z^{(i+1)} - Z^{(i)}} \log \frac{1}{Z^{(i+1)} - Z^{(i)}} dz \\
 &= - \sum_{i=0}^N \frac{1}{Z^{(i+1)} - Z^{(i)}} \log \frac{1}{Z^{(i+1)} - Z^{(i)}} \int_{Z^{(i)}}^{Z^{(i+1)}} dz \\
 &= - \frac{1}{N+1} \sum_{i=0}^N \log \frac{1}{Z^{(i+1)} - Z^{(i)}} \\
 &\stackrel{(b)}{\approx} - \frac{1}{N-1} \sum_{i=1}^{N-1} \log \frac{1}{Z^{(i+1)} - Z^{(i)}} \\
 &= \frac{1}{N-1} \sum_{i=1}^{N-1} \log \left((N+1)(Z^{(i+1)} - Z^{(i)}) \right) \\
 &\equiv \hat{H}_{simple}(Z^1, \dots, Z^N). \tag{5}
 \end{aligned}$$

The approximation (a) arises by approximating the true density $p(z)$ by $\hat{p}(z; Z^1, \dots, Z^N)$. The approximation (b) stems from the fact that in general we do not know $Z^{(0)}$ and $Z^{(N+1)}$, i.e. the true support of the unknown density. Therefore, we form the mean log density estimate using only information from the region for which we have some information, ignoring the intervals outside the range of the sample. This is equivalent to assuming that outside the sample range, the true density has the same mean log probability density as the rest of the distribution.

2.2 Lowering the Variance of the Estimate

While the estimate (5) has both intuitive and theoretical appeal, it suffers from high variance which it inherits from the variance of the interval probabilities (4).⁴ The upper left plot of Figure 1 shows the distribution of values obtained when we divide a random 1-spacing by its expected value. Clearly, these values are widely distributed around the ideal value of 1. This problem can be mitigated (and asymptotically eliminated) by considering m -spacing estimates of entropy, such as

$$\hat{H}_{m\text{-spacing}}(Z^1, \dots, Z^N) \equiv \frac{m}{N-1} \sum_{i=0}^{\frac{N-1}{m}-1} \log \left(\frac{N+1}{m} (Z^{m(i+1)+1} - Z^{mi+1}) \right). \tag{6}$$

Under the conditions that

$$m, N \rightarrow \infty, \frac{m}{N} \rightarrow 0, \tag{7}$$

4. The addition of a small constant renders this estimator weakly consistent for bounded densities under certain tail conditions (Hall, 1984).

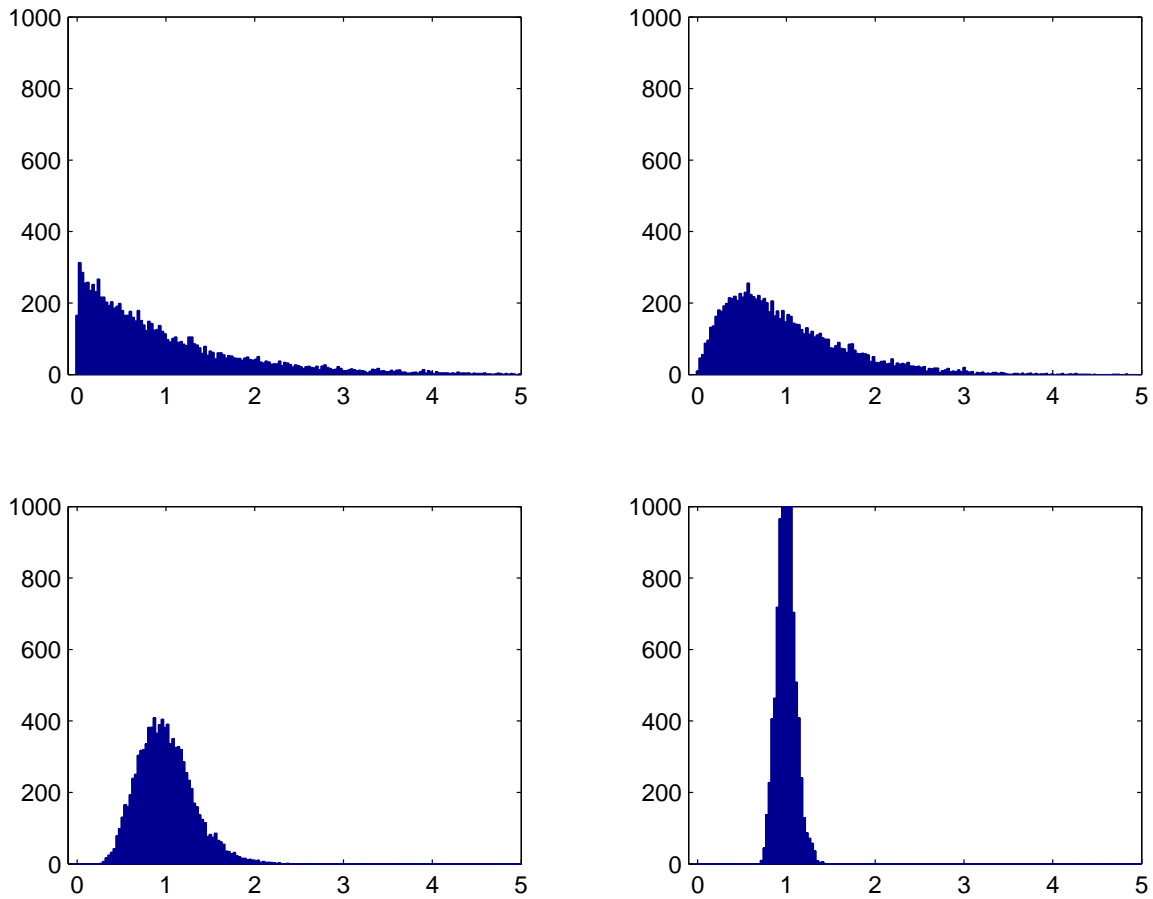


Figure 1: Histograms showing the variability of the probability mass of m -spacings, as a function of m . Each plot shows, for a particular m , the ratio of a set of random m -spacings to their expected values. When $m = 1$ (upper left plot), the probability mass of the m -spacings is widely distributed. Already for $m = 2$ (upper right), the ratio is substantially more concentrated around its expected value of 1. For $m = 10$ (lower left), the m -spacings' probability masses are almost always within a factor of three of their expected values. For $m = 100$ (lower right), the probability mass of the m -spacings is highly consistent. This behavior is a simple consequence of the law of large numbers and the uniformity of the distribution obtained through the probability integral transform.

this estimator also becomes consistent (Vasicek, 1976, Beirlant et al., 1997). In this work, we typically set $m = \sqrt{N}$.

The intuition behind this estimator is that by considering m -spacings with larger and larger values of m , the variance of the probability mass of these spacings, relative to their expected values, gets smaller and smaller. In fact, the probability mass of m -spacings is distributed according to a beta distribution with parameters m and $N + 1 - m$ (c.f. Arnold et al., 1992). The expectation of this distribution is $\frac{m}{N+1}$ and the variance is $\frac{m(N+1-m)}{(N+1)^2(N+2)}$. The ratio of the variance to the expectation is then $\frac{N+1-m}{(N+1)(N+2)}$, and we can see that this ratio drops linearly as m increases. This behavior is illustrated in Figure 1. Each plot shows, for a different value of m , the distribution of the ratio between random m -spacings and their expected value. The upper left plot shows that for $m = 1$, this distribution is distributed very widely. As m grows, the probability mass for each m -spacing concentrates around its expected value.

Such plots, which are functions of the probability mass of intervals defined by order statistics, have the same form for *all probability distributions with continuous cumulative distribution functions*. That is, the form depends only on the value of m and not at all on the probability law. This is again a consequence of the uniformity in distribution of the probability integral transform for any (impulse-free) density.

A modification of (6) in which the m -spacings overlap,⁵

$$\hat{H}_{\text{RADICAL}}(Z^1, \dots, Z^N) \equiv \frac{1}{N-m} \sum_{i=1}^{N-m} \log \left(\frac{N+1}{m} (Z^{i+m} - Z^{(i)}) \right), \quad (8)$$

is used in RADICAL. This is equivalent asymptotically to the estimator (3) of Vasicek (1976). Weak and strong consistency have been shown by various authors under a variety of general conditions assuming (7). For details of these results, see the review paper by Beirlant et al. (1997). Perhaps the most important property of this estimator is that it is asymptotically efficient, as shown by Levit (1978).

It is interesting to remark that while (5) and (6) have a natural correspondence to density estimates (if we ignore the region outside the range of the samples), there is no trivial correspondence between (8) and a density estimate. We are thus solving the entropy estimation problem without demanding that we solve the density estimation problem.⁶

We note that Pham (2000) defined an ICA contrast function as a sum of terms very similar to (6). However, by choosing $m = 1$ as was done in that work, one no longer obtains a consistent estimator of entropy, and the efficiency and efficacy of (6) as an ICA contrast function appears to be greatly reduced. In particular, much of the information about whether or not the marginals are independent is ignored in such an approach.

3. RADICAL in Two Dimensions

Given that we have an entropy estimate in hand, we now discuss its application to optimizing Equation (2). We first discuss aspects of the estimator in the context of the two-dimensional ICA problem. Later we will extend the optimization method to multiple dimensions. Two issues which arise and

5. Allowing the m -spacings to overlap reduces the asymptotic variance of the estimator.

6. For those who are skeptical that this is possible, we suggest that it is no different than estimating the variance of a random variable without estimating its density.

which must be dealt with are local minima and what we will refer to as “false minima”. The first issue is intrinsic to the optimization criterion (even in the case of infinite data) and appears difficult to address without adopting an exhaustive search strategy. The second is a function of the estimator and will motivate a smoothing approach. We address these issues by way of some canonical examples before proceeding to a more detailed discussion of the algorithm.

3.1 Examples

We illustrate various aspects of the estimator and the optimization procedure by separating three different types of mixed sources: (1) two uniform densities, (2) two double-exponential densities, and (3) two bi-modal Gaussian mixture densities. For each example, we examine 150 equally spaced rotations of the data between 0 and 90 degrees.

Consider Figure 2 which shows some results from separating a mixture of two uniform densities. Figure 2(a) shows the results over 100 Monte Carlo trials in which $N = 250$ and $m = 16 \approx \sqrt{250}$. As can be seen, the mean estimate (over 90 degrees of rotation) is fairly smooth with a clear global maximum at 45 degrees and a minimum at 0 degrees rotation (or equivalently at 90 degrees). However, not surprisingly, any one trial has several false local minima and maxima. In Figure 2(a), for example, the individual trials which exhibited the largest positive and negative deviation from the average (for any single angle θ) over all trials are overlaid on the average result. Similar figures for the other two cases are shown in Figures 3(a) and 4(a), although local minima and maxima (over individual trials)) are not as severe in these cases.

In particular, false minima can become quite severe when the sample size is small. They are a consequence of the fact that the m -spacings estimator makes no prior smoothness assumptions (e.g. limited spatial frequency) regarding the underlying densities. Consequently, for small sample size there exist rotations (instances of W) for which portions of the data spuriously approximately align, producing an artificial spike in one of the marginal distributions. This is most easily understood by considering the case in which m , the number of intervals combined in an m -spacing, is equal to 1. In this case, for any value of N there are many rotations ($O(N^2)$ of them, in fact) which will cause two points to align exactly, either vertically or horizontally. This causes the 1-spacing corresponding to these two points to have width 0 in one of the empirical marginal distributions, which in turn gives this interval an average logarithm of $-\infty$. This results in a marginal entropy estimate of $-\infty$ for this particular rotation of the data. The entropy estimator has no evidence that there is not, in fact, an impulse in the true marginal density which would legitimately indicate a negatively infinite entropy, so it is not a fundamental flaw with the estimator. Rather, it is a consequence of allowing arbitrarily peaked implicit marginal estimates. While this issue becomes less of a problem as N and m grow, our empirical findings suggest that for the densities considered in this paper (see Figure 6), it must be addressed to achieve optimal performance at least while $N \leq 2000$.

To address this problem, we consider a smoothed version of the estimator. We attempt to remove such false minima by synthesizing R replicates of each of the original N sample points with additive spherical Gaussian noise to make a surrogate data set X' . That is, each point X^j is replaced with R samples from the distribution $N(X^j, \sigma_r^2 I)$, where R and σ_r^2 become parameters of the algorithm. We refer to this as *augmenting* the data set X . Then we use the entropy estimator (8) on the augmented data set X' . R was chosen to have a value of 30 for most of the experiments in this report. Results of this modification to the estimator are shown in Figures 2(b), 3(b) and 4(b). While not completely

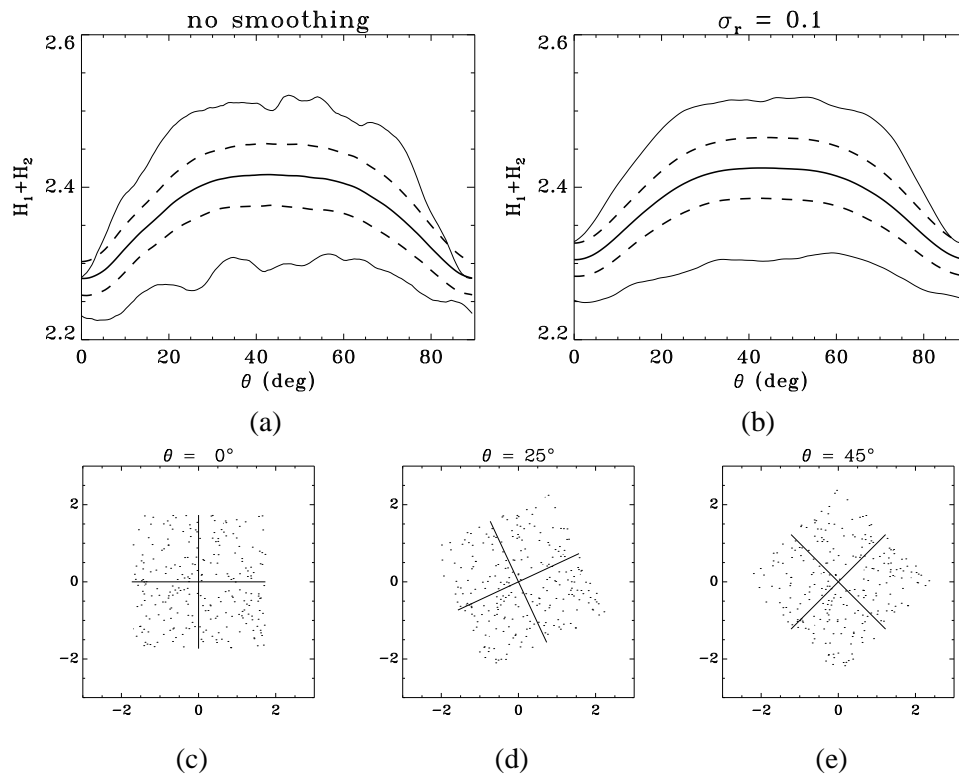


Figure 2: RADICAL for a mixture of two uniform densities. (a) The thick solid curve is the mean estimate of Equation (2) over 100 Monte Carlo trials with no data augmentation. The dotted curves indicate plus or minus one standard deviation, while the thinner (less smooth) curves are the two trials which had the largest positive and negative deviation from the mean respectively. (b) is exactly the same as (a) except that the data set was augmented with $R = 30$ and a smoothing factor of $\sigma_r = 0.1$ was used. (c) is one realization of the original sources with no rotation, (d) with 25 degrees rotation, and (e) with 45 degrees rotation. Axes of rotation are overlaid on the plots.

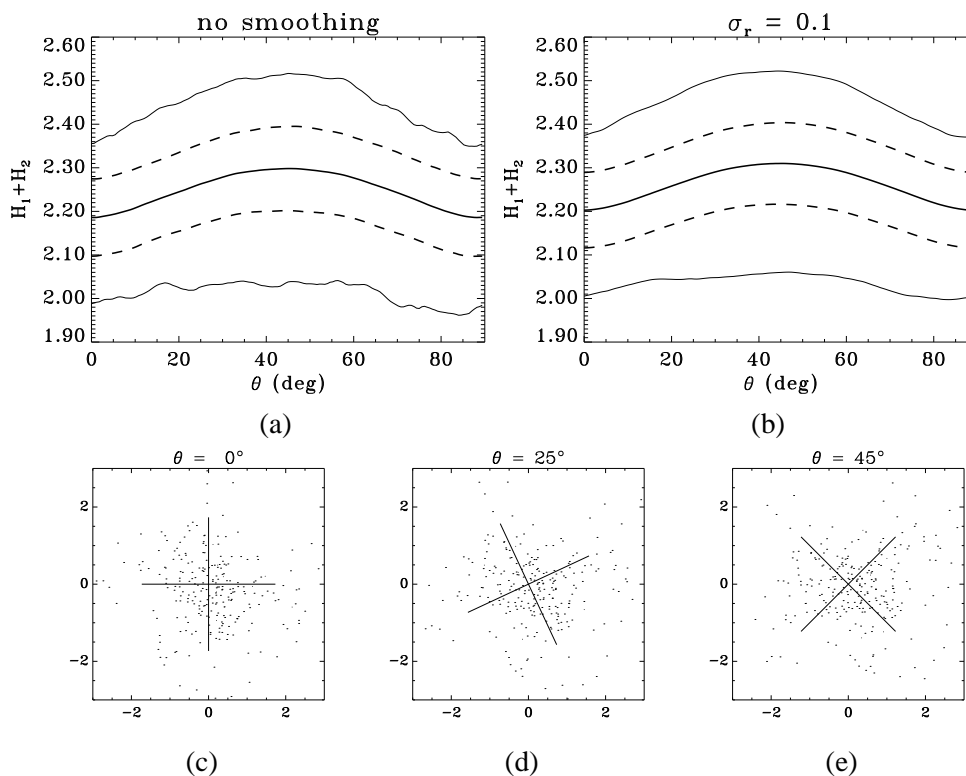


Figure 3: RADICAL for a mixture of two double-exponential densities. (a) The thick solid curve is the mean estimate of Equation (2) over 100 Monte Carlo trials with no data augmentation. The dotted curves indicate plus or minus one standard deviation, while the thinner (less smooth) curves are the two trials which had the largest positive and negative deviation from the mean respectively. (b) is exactly the same as (a) except that the data set was augmented with $R = 30$ and a smoothing factor of $\sigma_r = 0.1$ was used. (c) is one realization of the original sources with no rotation, (d) with 25 degrees rotation, and (e) with 45 degrees rotation. Axes of rotation are overlaid on the plots.

eliminating the problem of local minima and maxima, the results over the worst two trials are significantly smoother.

While we leave a rigorous analysis of this smoothing procedure for future work, we note the following important intuitions about it. The data augmentation procedure described allows the sampling of an arbitrary number of points from a density which is equal to the empirical distribution convolved with a Gaussian. This is similar, though not identical, to the true joint distribution convolved with this same Gaussian. It is easily shown that convolution of a joint distribution (of mixed components) with a spherical Gaussian does not change the solution to an ICA problem in the case of infinite data. Hence, the augmentation procedure allows the sampling of additional points from a distribution that is close to a distribution with the same solution as the original distribution. Because

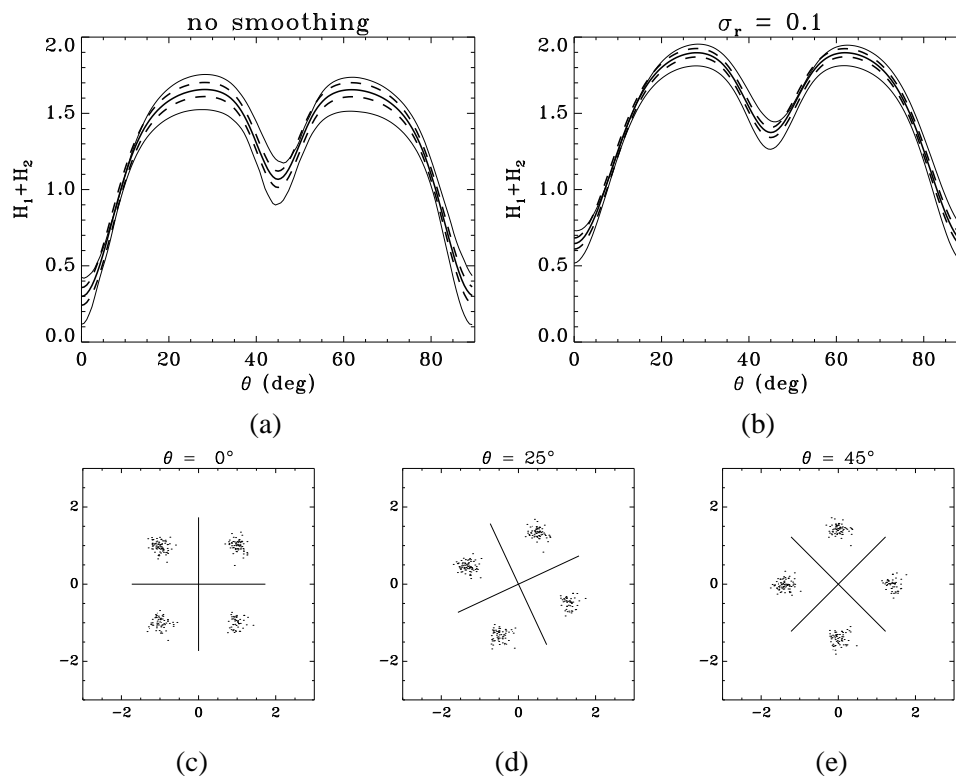


Figure 4: RADICAL for a mixture of two bi-modal densities. (a) The thick solid curve is the mean estimate of Equation (2) over 100 Monte Carlo trials with no data augmentation. The dotted curves indicate plus or minus one standard deviation, while the thinner (less smooth) curves are the two trials which had the largest positive and negative deviation from the mean respectively. (b) is exactly the same as (a) except that the data set was augmented with $R = 30$ and a smoothing factor of $\sigma_r = 0.1$ was used. (c) is one realization of the original sources with no rotation, (d) with 25 degrees rotation, and (e) with 45 degrees rotation. Axes of rotation are overlaid on the plots.

the sampling of additional points allows us to effectively increase m , it also allows the reduction of spurious local minima.

After reducing the effect of false minima on the optimization of W , we must still address legitimate local minima, the best example of which is shown in Figure 4 where a rotation of 45° is a true local minimum of the objective function. For two-dimensional source separation, taking advantage of the fact that $W(\theta)$ is a one-dimensional manifold, we do an exhaustive search over W for K values of θ . Note that we need only consider θ in the interval $[0, \frac{\pi}{2}]$, since any 90 degree rotation will result in equivalent independent components. In all of our experiments, we set $K = 150$. Importantly, it turns out that even in higher dimensions, our algorithm will remain linear in K (although polynomially more expensive in other respects), so it is relatively inexpensive to do a finer grain search over θ if desired. Complexity issues will be discussed in more detail below.

3.2 The ICA Algorithm

RADICAL is a very simple algorithm. Assuming that our observed data have already been whitened, there are really only two remaining steps. The first is to generate an augmented data set X' from X by the procedure described in the previous section. The second is to minimize the cost function (2), which we do by exhaustive search. Various aspects of RADICAL are summarized in Figure 5.

There are four parameters with which we experimented informally in our early experiments. The first parameter m , determines the number of intervals combined in an m -spacing. As stated above, we chose $m = \sqrt{N}$ for all of our experiments, which guarantees the asymptotic consistency of our procedure as long as none of the marginal densities have impulses. When condition (7) is satisfied, the entropy estimator will be consistent and should perform well for large N . For small N , performance can be improved by choosing m according to the particulars of the distribution, but since the distribution is unknown in general, we avoided this and chose a fixed rule for m as a function of N for all of our experiments.

A second parameter is the number of points R used to replace each original point X^j when creating the augmented data set. The value of R can be made smaller for large N , and as N and m get large enough, point replication is entirely unnecessary, since the optimization landscape will eventually become smooth (to within the resolution of the search algorithm). However, at $N = 4000$, the largest value with which we experimented, point replication was still necessary. The experiments in this paper all used a value of $R = 30$, irrespective of the original sample size N .

Next we examine σ_r^2 , the variance of the R added points for each of the N points X^j . As expected, from informal testing, we found that performance was somewhat better if we allowed the variance to shrink as N grew. However, performance was relatively robust to the choice of this parameter and we chose only two different values of σ_r for all of our experiments. For $N < 1000$, we set $\sigma_r = 0.35$ and for $N \geq 1000$, we halved this value, setting $\sigma_r = 0.175$.

The only remaining parameter for RADICAL in two dimensions is K , the number of rotations at which to measure the objective function. We experimented with values of 50, 100, 150, and 250. There was no noticeable improvement in performance for $K > 150$, even for $N = 4000$ and the higher dimensional tests. Of course, with N large enough, one could benefit to some extent by increasing K . Since in two dimensions, the error metric (see below) is proportional to the difference in angle between the estimated θ and the optimal θ , it is easy to see that asymptotically, the expected error is a function of K and is approximately

$$\frac{1}{2} \frac{\pi}{K} = \frac{\pi}{4K}.$$

For $K = 150$, this asymptotic expected error is approximately 0.005, a number small enough to be only a minor contribution to the total error (see experiments) for values of N considered here. Since both the two-dimensional and higher-dimensional versions of RADICAL are linear in K , it is relatively inexpensive to increase the resolution of the exhaustive search.

3.3 Algorithmic Complexity

An upper bound on the algorithmic complexity of RADICAL in two dimensions is fairly straightforward to compute. There are a number of opportunities for speedup which we will leave for future work. We will assume for this analysis and for the higher dimensional case discussed later that D , the dimension, is less than N , the sample size.

Algorithm:	RADICAL, two-dimensional version.
Input:	Data vectors X^1, X^2, \dots, X^N , assumed whitened.
Parameters:	m : Size of spacing. Usually equal to \sqrt{N} . σ_r^2 : Noise variance for replicated points. R : Number of replicated points per original data point. K : Number of angles at which to evaluate cost function.
Procedure:	<ol style="list-style-type: none"> 1. Create X' by replicating R points with Gaussian noise for each original point. 2. For each θ, rotate the data to this angle ($Y = W(\theta) * X'$) and evaluate cost function. 3. Output the W corresponding to the optimal θ.
Output:	W , the demixing matrix.

Figure 5: A high-level description of RADICAL for the two-dimensional ICA problem.

We assume that the data has been whitened to begin with. Whitening the data is $O(D^2N)$. In two dimensions, we will treat D as a constant, giving an $O(N)$ operation. Augmenting the data set with R noisy copies of each point is just $O(NR)$. Let $N' = NR$ be the size of the augmented data set. Rotation of the augmented data points to an angle θ by matrix multiplication is at most $O(D^2N')$, but again for fixed D , we can call D^2 a constant, so this reduces to $O(N')$. In two dimensions, our estimator requires two one-dimensional sorts, taking time $O(N' \log N')$, and two sums over at most N' spacings, which is $O(N')$. Thus, evaluating the objective function once, which involves matrix multiplication, sorting, and summing, takes time $O(N') + O(N' \log N') + O(N') = O(N' \log N')$. Note that m , the spacing size, does not enter into the complexity of evaluating the objective function.

We repeat this procedure K times in our exhaustive search. This gives us an upper bound of $O(KN' \log N')$ for the minimization of the objective function. For the whole algorithm, including whitening, we then have $O(N) + O(KN' \log N') = O(N) + O(KNR \log(NR)) = O(KNR \log(NR))$ as the final complexity for the two-dimensional algorithm. As mentioned previously, it should be possible to reduce R to 1 for large N , so technically, we can claim that RADICAL is $O(KN \log N)$. However, for moderate and low values of N , we must still choose $R > 1$, and so we include it in our complexity analysis.

3.4 Experiments in Two Dimensions

To test the algorithm experimentally, we performed a large set of experiments, largely drawn from the comprehensive tests developed by Bach and Jordan (2002). Our tests included comparisons with FastICA (Hyvärinen and Oja, 1997), the JADE algorithm (Cardoso, 1999b), the extended Infomax algorithm (Lee et al., 1999b), and two versions of KernelICA: KCCA and KGV (Bach and Jordan, 2002). For each of the 18 one-dimensional densities shown in Figure 6, which were normalized to have zero mean and unit variance, the following experiments were performed. Using a density $q(\cdot)$, N points were drawn iid from the product distribution $q(\cdot)q(\cdot)$. The points were then subjected to a random rotation matrix A to produce the input X for the algorithm.⁷ We then measured the “difference” between the true matrix A and the W returned by the algorithm, according to the well-

7. Alternatively, we could have applied a random non-singular matrix to the data, and then whitened the data, keeping track of the whitening matrix. For the size of N in this experiment, these two methods are essentially equivalent.

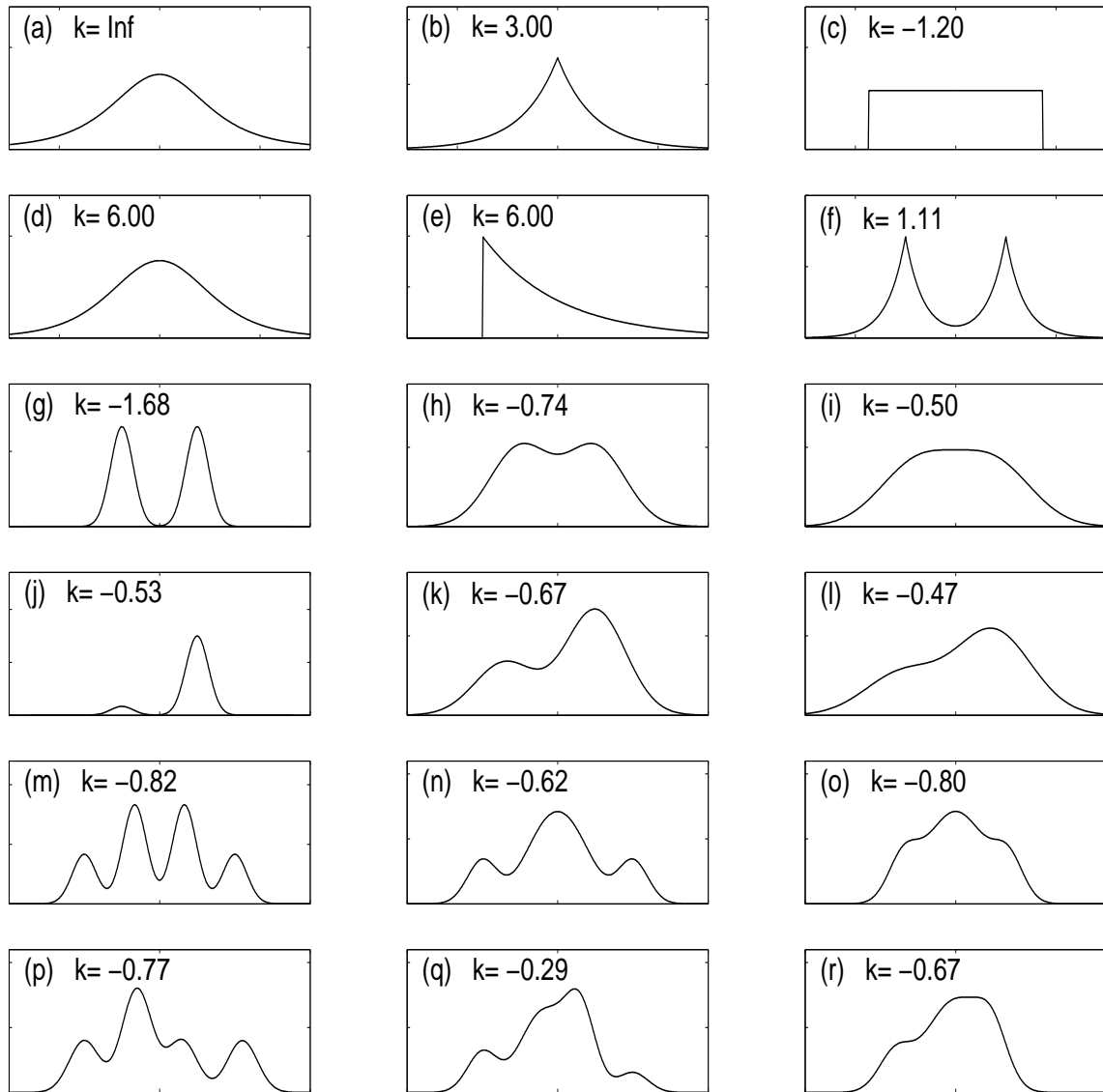


Figure 6: Probability density functions of sources with their kurtoses: (a) Student with three degrees of freedom; (b) double exponential; (c) uniform; (d) Student with five degrees of freedom; (e) exponential; (f) mixture of two double exponentials; (g)-(h)-(i) symmetric mixtures of two Gaussians: multimodal, transitional and unimodal; (m)-(n)-(o) symmetric mixtures of four Gaussians: multimodal, transitional and unimodal; (p)-(q)-(r) nonsymmetric mixtures of four Gaussians: multimodal, transitional and unimodal. This figure and code to sample from these distributions was generously provided by Francis Bach, UC Berkeley.

pdfs	FastICA	Jade	Imax	KCCA	KGV	RADICAL
a	8.9	7.5	56.3	6.6	5.7	5.6
b	10.2	9.3	61.8	8.4	6.2	7.0
c	4.4	3.1	18.4	4.7	4.3	2.4
d	11.8	10.0	61.1	13.1	11.6	12.6
e	8.1	7.4	67.7	3.7	3.1	1.7
f	7.9	5.5	12.4	3.6	3.3	2.0
g	3.9	2.9	18.1	3.1	2.9	1.4
h	11.1	8.2	27.2	10.8	8.4	12.1
i	18.5	16.7	37.6	25.2	23.2	27.0
j	12.2	12.8	50.5	3.1	3.0	1.7
k	14.1	10.3	30.2	6.1	5.2	5.5
l	22.6	16.4	39.2	10.6	8.7	11.7
m	8.2	6.9	29.5	14.8	12.3	1.9
n	11.4	9.7	32.1	16.3	9.7	3.9
o	8.7	6.8	23.7	13.0	9.4	8.6
p	9.9	6.7	29.1	7.7	6.0	2.6
q	35.8	32.0	39.1	12.4	9.4	5.3
r	13.0	9.5	27.7	9.7	7.2	8.9
mean	12.3	10.1	36.8	9.6	7.8	6.8
rand	10.7	8.5	29.6	8.3	6.0	5.8

Table 1: The Amari errors (multiplied by 100) for two-component ICA with 250 samples. For each density (from a to r), averages over 100 replicates are presented. For each distribution, the lowest error rate is shown in bold face. The overall mean is calculated in the row labeled **mean**. The **rand** row presents the average over 1000 replications when two (generally different) densities were chosen uniformly at random among the 18 possible densities.

known criterion, due to Amari et al. (1996):

$$d(A, W) = \frac{1}{2D} \sum_{i=1}^D \left(\frac{\sum_{j=1}^D |b_{ij}|}{\max_j |b_{ij}|} - 1 \right) + \frac{1}{2D} \sum_{j=1}^D \left(\frac{\sum_{i=1}^D |b_{ij}|}{\max_i |b_{ij}|} - 1 \right),$$

where $b_{ij} = (AW^{-1})_{ij}$. Table 1 shows the mean results for each source density on each row, with $N = 250$, the number of input points, and 100 replications of each experiment. The best performing algorithm on each row is shown in bold face. Note that RADICAL performs best in 10 of 18 experiments, substantially outperforming the second best in many cases. The mean performance in these experiments is shown in the row labeled **mean**, where RADICAL has lower error than all other algorithms tested. The final row of the table represents experiments in which two (generally different) source densities were chosen randomly from the set of 18 densities to produce the product distribution from which points were sampled. 1000 replications were performed using these randomly chosen distributions. For these experiments, RADICAL has a slight edge over Kernel-ICA, but they both significantly outperform the other methods.

pdfs	FastICA	Jade	Imax	KCCA	KGV	RADICAL
a	4.4	3.7	1.8	3.7	3.0	2.1
b	5.8	4.1	3.4	3.7	2.9	2.7
c	2.3	1.9	2.0	2.7	2.4	1.2
d	6.4	6.1	6.9	7.1	5.7	5.3
e	4.9	3.9	3.2	1.7	1.5	0.9
f	3.6	2.7	1.0	1.7	1.5	1.0
g	1.8	1.4	0.6	1.5	1.4	0.6
h	5.1	4.1	3.1	4.6	3.6	3.7
i	10.0	6.8	7.8	8.3	6.4	8.3
j	6.0	4.5	50.6	1.4	1.3	0.8
k	5.8	4.4	4.2	3.2	2.8	2.7
l	11.0	8.3	9.4	4.9	3.8	4.2
m	3.9	2.8	3.9	6.2	4.7	1.0
n	5.3	3.9	32.1	7.1	3.0	1.8
o	4.4	3.3	4.1	6.3	4.5	3.4
p	3.7	2.9	8.2	3.6	2.8	1.1
q	19.0	15.3	43.3	5.2	3.6	2.3
r	5.8	4.3	5.9	4.1	3.7	3.2
mean	6.1	4.7	10.6	4.3	3.3	2.6
rand	5.1	4.1	6.8	3.1	2.0	2.1

Table 2: The Amari errors (multiplied by 100) for two-component ICA with 1000 samples. For each probability density function (from a to r), averages over 100 replicates are presented. The overall mean is calculated in the row labeled **mean**. The **rand** row presents the average over 1000 replications when two (generally different) densities were chosen uniformly from random among the 18 possible densities.

Table 2 shows an analogous set of results for larger data sets, with $N = 1000$. Again, RADICAL outperforms the other algorithms for most densities. However, Kernel-ICA outperforms RADICAL by a small margin in the randomized experiments.

3.5 Robustness to Outliers

Figure 7 shows results for our outlier experiments. These experiments were again replications of the experiments performed by Bach and Jordan (2002). Following Bach and Jordan, we simulated outliers by randomly choosing up to 25 data points to corrupt. This was done by adding the value +5 or -5 (chosen with probability 1/2) to a single component in each of the selected data points, *after the data was whitened*. We performed 100 replications using source distributions chosen uniformly at random from the 18 possible sources. It can be seen that RADICAL is uniformly more robust to outliers than all other methods in these experiments, for every number of outliers added.

Whitening of data, however, is itself a challenging problem in the presence of outliers. Because it was assumed that the data was whitened before outliers were added, these experiments should be taken mainly as an indicator that the estimator of entropy is robust to outliers, rather than that RADICAL itself can be applied to a raw sample in the presence of outliers. The success in these experiments suggests that the coupling of RADICAL with a robust scheme for whitening a sample may produce a more practical algorithm for ICA in the presence of outliers.

4. RADICAL in D Dimensions

Clearly RADICAL will be more useful if it can be applied in higher dimensions than $D = 2$. While projections and rotations of high dimensional data present no challenge, one might worry that our objective function is difficult to minimize considering the complexity of computing the gradient of our entropy estimator.⁸ Additionally, it is known all too well that exhaustive search in more than a few dimensions is infeasible, as its complexity is $O(N^D)$, where N must be large to insure accuracy. It turns out, however, that for the ICA problem, the minimization can still be approached in an “exhaustive” manner. Successive minimizations along different pairs of dimensions works well. That is, we can recast the D -dimensional ICA problem as a series of two-dimensional ICA problems, which we can solve well. Empirically, we show that for dimensions as high as 16, RADICAL on average outperforms or performs similarly to all other algorithms against which we tested it.

4.1 Jacobi Rotations

To find the D -dimensional rotation matrix W^* that optimizes (2) in D dimensions, we use Jacobi methods such as those used to by Comon (1994) in the ICA problem or to solve symmetric eigenvalue problems (c.f. Golub and Van Loan, 1996). The basic idea is to rotate the augmented data X' two dimensions at a time using what are known as *Jacobi rotations*.⁹ A Jacobi rotation of angle θ

8. Technically, the estimator *is* differentiable since it is locally smooth. However, evaluation of the gradient at each iteration would require a sorting step.

9. Jacobi rotations are also known as *Givens rotations*.

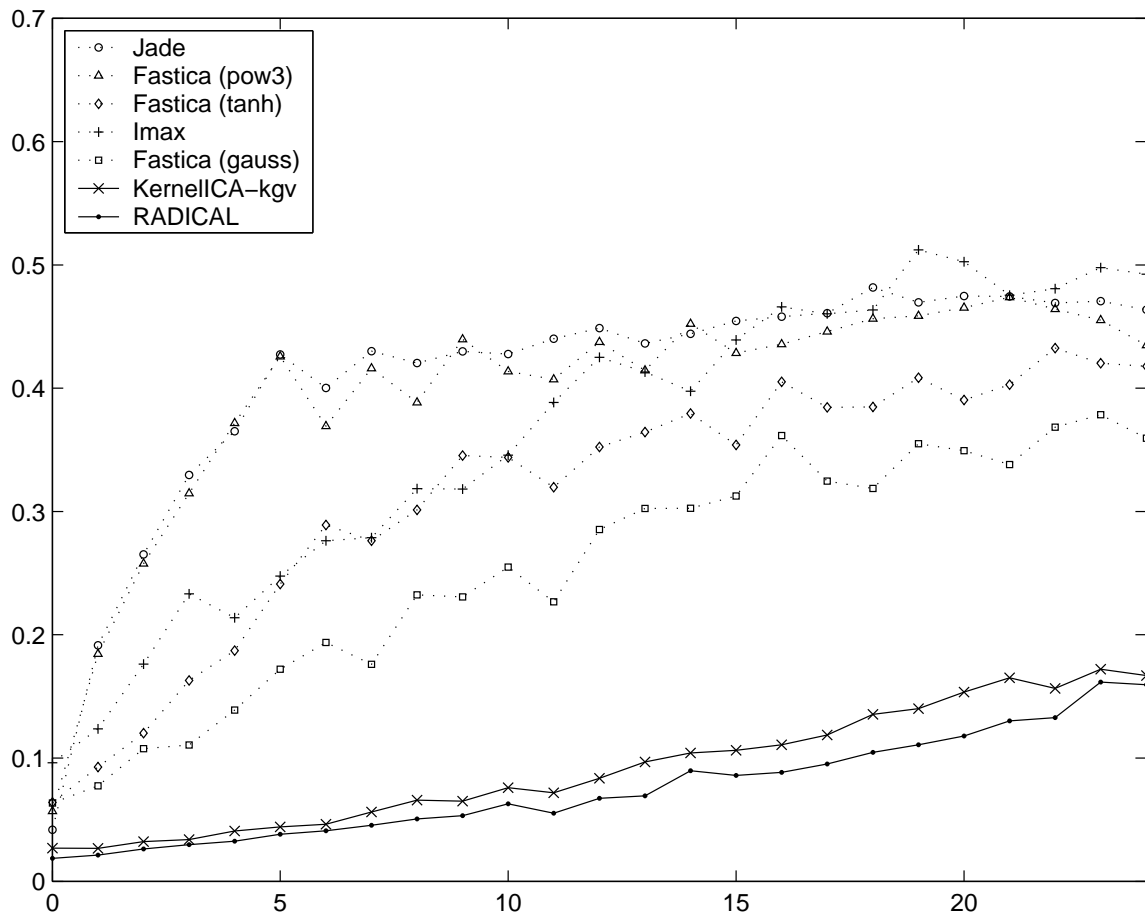


Figure 7: Robustness to outliers. The abscissa displays the number of outliers and the ordinate shows the Amari error.

for dimensions p and q is defined as

$$J(p, q, \theta) = \begin{bmatrix} 1 & \cdots & 0 & \cdots & 0 & \cdots & 0 \\ \vdots & \ddots & \vdots & & \vdots & & \vdots \\ 0 & \cdots & \cos(\theta) & \cdots & -\sin(\theta) & \cdots & 0 \\ \vdots & & \vdots & \ddots & \vdots & & \vdots \\ 0 & \cdots & \sin(\theta) & \cdots & \cos(\theta) & \cdots & 0 \\ \vdots & & \vdots & & \vdots & \ddots & \vdots \\ 0 & \cdots & 0 & \cdots & 0 & \cdots & 1 \end{bmatrix},$$

where the sines and cosines appear on the p th and q th rows and columns of the matrix. Since a Jacobi rotation leaves all components of a D -dimensional data point X^j unchanged except for the p th and q th components, optimizing our objective function (2) reduces to a two-dimensional ICA problem for each distinct Jacobi rotation.

Algorithmically, we initialize Y to our augmented data set X' , and our rotation matrix W to the identity matrix. After optimizing our objective function for a pair of dimensions (p, q) , we update Y :

$$Y_{new} = J(p, q, \theta^*)Y,$$

keeping track of our cumulative rotation matrix:

$$W_{new} = J(p, q, \theta^*)W.$$

Note that since each Jacobi rotation affects only two components of Y , this is an $O(2^2NR) = O(NR)$ operation. Thus, full scale D -dimensional rotations need never be done (all at once). This is discussed further below.

There are $D(D-1)/2$ distinct Jacobi rotations (parameterized by θ), and optimizing over a set of these is known as a *sweep*. Empirically, performing multiple sweeps improves our estimate of W^* for some number of iterations, and after this point, the error may increase or decrease sporadically near its smallest value. The number of sweeps S becomes an additional parameter for multi-dimensional RADICAL. We found that $S \approx D$ provided good results for all of our multi-dimensional experiments.

4.2 Complexity of RADICAL in D Dimensions

The complexity of RADICAL in D dimensions is again straightforward. Starting with the whitening of the data, we must now spend $O(D^2N)$ time on this step. Of course, we can no longer legitimately treat the dimension D as a constant. Producing the augmented data set X' now becomes an $O(DNR)$ procedure, but this will be dominated by other terms.

A single sweep through $D(D-1)/2$ Jacobi rotations produces a complexity increase by a factor of $O(D^2)$ for a total sweep complexity of $O(K(D^2)N' \log N')$. Recall that $N' = NR$ is the size of the augmented data set. The number of sweeps necessary for convergence is difficult to predict, but it seldom exceeded the dimension D . Including the number of sweeps in the complexity gives $O(SK(D^2)N' \log N')$.

We note that this complexity analysis includes the optimization, so it should be compared against the *total run time* of other algorithms, not simply the time to evaluate the objective function or

Algorithm:	RADICAL, D -dimensional version.
Input:	Data vectors X^1, X^2, \dots, X^N , assumed whitened.
Parameters:	m : Size of spacing. Usually equal to \sqrt{N} . σ_r^2 : Noise variance for replicated points. R : Number of replicated points per original data point. K : Number of angles at which to evaluate cost function. S : Number of sweeps for Jacobi rotations.
Procedure:	<ol style="list-style-type: none"> 1. Create X' by replicating R points with Gaussian noise for each original point. 2. For each of S sweeps (or until convergence): <ol style="list-style-type: none"> a. For each of $D(D-1)/2$ Jacobi rotations for dimensions (p, q): <ol style="list-style-type: none"> i. Perform 2-D RADICAL, returning optimal $J(p, q, \theta^*)$. ii. Update Y according to $Y_{new} = J(p, q, \theta^*)Y$. iii. Update W according to $W_{new} = J(p, q, \theta^*)W$. 3. Output final W.
Output:	W

Figure 8: A high-level description of RADICAL for D dimensions.

compute a derivative. Most other algorithms use a gradient descent procedure, potentially getting trapped in local minima that can be circumvented using the one-dimensional exhaustive search of RADICAL. If randomized restarts are used by other algorithms to escape these minima, then of course this must be factored into the complexity analysis.

Before moving on to the experimental results of RADICAL in D dimensions, we make the following observations regarding the specifics of optimization in the ICA problem:

1. One reason that an exhaustive search approach is feasible for the two-dimensional problem is that the domain of the unknown rotation parameter θ is bounded, i.e. it is $[0, \frac{\pi}{2}]$. In multiple dimensions, this property continues to hold. This makes the pre-whitened ICA problem different from optimization problems over infinite domains, such as \mathfrak{R}^N , where sampling the parameter domain in a dense fashion is not possible.
2. Typically, in a multidimensional optimization problem, the optimization of one parameter cannot be performed independently of another parameter. Due to the special nature of the optimization criterion (the sum of marginal entropies), however, the Jacobi rotations have the interesting property that collections of them are independent of each other. That is, adjusting the cumulative rotation matrix via a multiplication by $J(p_1, q_1, \theta_1^*)$ will not perturb the solution to a previous Jacobi rotation $J(p_2, q_2, \theta_2^*)$ if p_1, p_2, q_1 , and q_2 are all distinct. This is because most of the terms in the criterion to be optimized, the sum of marginal entropies, are not affected by a particular Jacobi rotation. In fact, exactly $D-2$ of them are not affected. This means that the optimization criterion is “almost factorized.” This “non-conflicting” structure has been observed before (c.f. Golub and Van Loan, 1996), and suggests that local minima may be easier to escape than in a typical multidimensional optimization problem, using the Jacobi strategy paired with an exhaustive search technique. Incidentally, this near factorization structure lends itself to parallel implementation (Golub and Van Loan, 1996).

3. It may appear that we chose an exhaustive search strategy because our entropy estimator is not easily differentiated. But in fact our main motivation for using an exhaustive search strategy is to escape local minima. Furthermore, we emphasize again that our algorithm is linear in K , irrespective of the dimension D . Thus, the exhaustive search remains one-dimensional even in the multidimensional problem, and hence is efficient, and even preferable to gradient descent due to its ability to escape (at least some) local minima.

Hence, while exhaustive search is often dismissed as less efficient than other methods, the special structure of this particular problem and our application of the method suggest it may have advantages over gradient descent.

RADICAL has higher computational complexity than some other ICA algorithms. However, efficiency must be considered in conjunction with efficacy. While RADICAL cannot be considered “efficient” relative to methods that make parametric assumptions about the data (they are $O(N)$ in the sample size vs. $O(N \log N)$), or relative to gradient descent methods that may be linear in the dimension (as opposed to quadratic), it is more ambitious than either of these classes. In particular, it is non-parametric and attempts to avoid local minima. It is fast enough to run experiments (in a few hours) on a single desktop machine in up to 16 dimensions, which make it substantially faster than algorithms such as Kernel ICA.¹⁰ Finally, RADICAL could probably benefit by starting from the solution of a faster algorithm and optimizing from there, a strategy we shall investigate in the future.

4.3 Results for D Dimensions

Table 3 presents results of experiments for multiple dimensions. In each experiment for dimension D , D (generally) different densities were selected at random from the set of 18 densities discussed above. Again this data was randomly rotated, and the task was to recover the independent components. Notice that RADICAL is either the best or second best performer in each case, performing better than all other algorithms in four of seven experiments.

5. Conclusions

We have presented a novel algorithm, RADICAL, for independent component analysis. Our approach was predicated on several principles. First, direct estimation of entropy obviates the need for density estimation as an intermediate step. Second, over the space of smooth densities there are unavoidable local minima in the commonly used K-L divergence based optimization landscape. This necessitated in some respects a global search over the parameter space in order to achieve good convergence properties over a broad set of source densities. Toward that end we employed a variant of the nonparametric entropy estimator of Vasicek (1976) which is both computationally efficient and robust. In addition, our algorithm is easily used in higher dimensions. Empirical results were reported for a significant number of 2-D separation problems, 2-D separation with outliers, and a range of multi-dimensional separation problems. Our empirical results demonstrated comparable or superior results (as measured by the Amari error) to a large number of well known algorithms.

While these initial results are promising, there is still room for improvement in the algorithms as presented from both a computational and theoretical perspective. On the computational side, we take no advantage of local changes in sorting order due to local changes in rotation. Consequently, the

10. Personal communication, Francis Bach.

dims	N	#repl	FastICA	Jade	Imax	KGV	RADICAL
2	250	1000	11	9	30	5	6
	1000	1000	5	4	7	2	2
4	1000	100	18	13	25	11	6
	4000	100	8	7	11	4	3
8	2000	50	26	22	123	20	11
	4000	50	18	16	41	8	8
16	4000	25	42	38	130	19	15

Table 3: Results for experiments in higher dimensions (again, mean Amari error multiplied by 100). The table shows experiments for dimensions two through 16. The number of points used for each experiment is shown in the second column and the number of experiment replications performed to obtain the mean values at right is given in the third column. KGV is Kernel-ICA using the kernel generalized variance. Note that RADICAL performed best or equal to best in all but one experiment.

application of standard sorting algorithms for such scenarios would be expected to greatly reduce the computational complexity of the analysis. From the theoretical perspective we presented a smoothed variant of the Vasicek estimator. Smoothing was accomplished via Monte Carlo techniques which might be avoided entirely (also reducing the computational complexity) by considering alternative methods for biasing the entropy estimate for smooth densities. Such will be the focus of our future efforts.

Finally, we have only considered the *noiseless* ICA problem as opposed to the common, and probably more realistic alternative model

$$X = AS + N,$$

where N is a vector random variable of noise added *after* the mixing. As currently formulated, we make no claims about the performance of RADICAL on data from such a generative model. Adapting RADICAL to such a model will be the subject of future work.

Acknowledgments

This work was greatly expedited and facilitated by the generous contributions of Francis Bach. He contributed code for experiments, and provided invaluable support in replicating the set of experiments developed in his previous work with Mike Jordan. We thank both of them for their help. We would also like to thank Bin Yu, David Brillinger, Andrew Ng, Jaimyoung Kwon, and Jon McAuliffe for helpful discussions. In addition, the reviewers made a variety of helpful comments and suggestions for which the authors are grateful.

The work of E. Learned-Miller was supported in part by ONR grant N00014-01-1-0890. The work of J. Fisher was supported in part by ODDR&E MURI Grant DAAD19-00-1-0466 through the ARO.

References

- S. Amari, A. Cichocki, and H. H. Yang. A new learning algorithm for blind signal separation. In D. S. Touretzky, M. C. Mozer, and M. E. Hasselmo, editors, *Advances in Neural Information Processing Systems*, 8. MIT Press, 1996.
- B. C. Arnold, N. Balakrishnan, and H.N. Nagaraja. *A First Course in Order Statistics*. John Wiley & Sons, 1992.
- F. R. Bach and M. I. Jordan. Kernel independent component analysis. *Journal of Machine Learning Research*, 3:1–48, 2002.
- J. Beirlant, E. J. Dudewicz, L. Györfi, and E. C. van der Meulen. Nonparametric entropy estimation: An overview. *International Journal of Mathematical and Statistical Sciences*, 6(1):17–39, June 1997.
- A. Bell and T. Sejnowski. An information maximization approach to blind separation and blind deconvolution. *Neural Computation*, 7:1129–1159, 1995.
- A. Benveniste, M. Goursat, and G. Ruget. Robust identification of a nonminimum phase system: blind adjustment of a linear equalizer in data communications. *IEEE Transactions on Automatic Control*, 25(3):385–99, 1980.
- J.-F. Bercher and C. Vignat. Estimating the entropy of a signal with applications. *IEEE Transactions on Signal Processing*, 48(6):1687–1694, 2000.
- J.-F. Cardoso. High-order contrasts for independent component analysis. *Neural Computation*, 11(1):157–192, 1999a.
- J.-F. Cardoso. High-order contrasts for independent component analysis. *Neural Computation*, 11(1):157–192, 1999b.
- J.-F. Cardoso and A. Souloumiac. Jacobi angles for simultaneous diagonalization. *SIAM Journal on Matrix Analysis and Applications*, 17(1):161–164, January 1996. ISSN 0895-4798 (print), 1095-7162 (electronic). URL <http://epubs.siam.org/sam-bin/dbq/article/25954>.
- P. Comon. Independent component analysis - a new concept? *Signal Processing*, 36:287–314, 1994.
- Thomas M. Cover and Joy A. Thomas. *Elements of Information Theory*. John Wiley & Sons, Inc., 1991.
- G. H. Golub and C. F. Van Loan. *Matrix Computations*. Johns Hopkins University Press, 1996.
- P. Hall. Limit theorems for sums of general functions of m-spacings. *Mathematical Proceedings of the Cambridge Philosophical Society*, 96:517–532, 1984.
- A. Hyvärinen. New approximations of differential entropy for independent component analysis and projection pursuit. In *Advances in Neural Information Processing Systems 10*, pages 273–279, 1997.

- A. Hyvärinen. Fast and robust fixed-point algorithms for independent component analysis. *IEEE Transactions on Neural Networks*, 10(3):626–634, May 1999.
- A. Hyvärinen. Blind source separation by nonstationarity of variance: A cumulant-based approach. *IEEE Transactions on Neural Networks*, 12(6):1471–1474, Nov 2001.
- A. Hyvärinen and E. Oja. A fast fixed point algorithm for independent component analysis. *Neural Computation*, 9(7):1483–1492, 1997.
- C. Jutten and J. Herault. Blind separation of sources, Part I: An adaptive algorithm based on neuromimetic architecture. *Signal Processing*, 24(1):1–10, 1991.
- S. Kullback. *Information Theory and Statistics*. John Wiley and Sons, 1959.
- T. Lee, M. Girolami, A. Bell, and T. Sejnowski. A unifying information-theoretic framework for independent component analysis. *International Journal on Mathematical and Computer Modeling*, 1999a.
- T.-W. Lee, M. Girolami, and T. J. Sejnowski. Independent component analysis using an extended Infomax algorithm for mixed sub-gaussian and super-gaussian sources. *Neural Computation*, 11(2):417–441, 1999b.
- B. Ya Levit. Asymptotically optimal estimation of nonlinear functionals. *Problems of Information Transmission*, 14:65–72, 1978.
- E. B. Manoukian. *Modern Concepts and Theorems of Mathematical Statistics*. Springer-Verlag, 1986.
- B.A. Pearlmutter and L.C. Parra. A context-sensitive generalization of ica. In *International Conference on Neural Information Processing*, Sep 1996.
- D.-T. Pham. Blind separation of instantaneous mixture of sources based on order statistics. *IEEE Transactions on Signal Processing*, 48(2):363–375, 2000.
- D.-T. Pham, P. Garrat, and C. Jutten. Separation of a mixture of independent sources through a maximum likelihood approach. In *Proceedings of EUSIPCO*, pages pages 771–774, 1992.
- C. E. Shannon. The mathematical theory of communication. *The Bell System Technical Journal*, 27:379–423,623–656, Jul,Oct 1948.
- O. Vasicek. A test for normality based on sample entropy. *Journal of the Royal Statistical Society, Series B*, 38(1):54–59, 1976.